# Movable insulation in building integrated semi-transparent photovoltaic thermal (BiSPVT) system



IOP Conf. Series: Materials Science and Engineering **556** (2019) 012052 doi:10.1088/1757-899X/556/1/012052

# Movable insulation in building integrated semi-transparent photovoltaic thermal (BiSPVT) system

**G K Mishra**[1*], **G N Tiwari**[2] and **T S Bhatti**[1]
[1]Center for Energy Studies, Indian Institute of Technology Delhi, New Delhi, India
[2]Bag Energy Research Society (BERS), Ghaziabad, India

E-mail: mishra.gourav@gmail.com (G K Mishra)

**Abstract.** The BiSPVT system involves an integration of semi-transparent photovoltaic (SPV) modules with buildings along with the provision of harvesting thermal energy. The system generates electrical and thermal energy for the building as well as provides day-lighting. However, during summer season the production of thermal energy is higher and thermal demand is lesser as compared to winter season. Also, the higher thermal energy production is unfavourable for the generation of electrical energy by SPV modules. The use of movable insulation (MI) on glazed wall can be one of the method to reduce the thermal energy generation. In this paper, a thermal model has been developed for BiSPVT system and the effect of MI on thermal performance of the system is studied. The energy balance equations are obtained for the inclined SPV modules (top), reinforced cement concrete (RCC) floor (bottom), air of room (SPV modules, floor and four brick/glazed side walls). The room temperature and SPV cell temperature are derived as a function of a) climatic parameters (solar irradiance and ambient temperature), b) design parameters and c) heat transfer coefficients by using the energy balance equations. It is found that by using MI with less or no air cavity thickness, the temperature of room has reduced by 1.93°C. However, the effect of MI on SPV cell temperature is marginal. The proposed model can be utilized to evaluate cell and room temperatures for BiSPVT system installed at different places of the world provided solar irradiance and ambient temperature of that place are known.

**Keywords:** Building integrated semi-transparent photovoltaic thermal (BiSPVT) system, Thermal modelling, Movable insulation, Photovoltaic system.

## 1. Introduction

The energy demand of building sector accounts for approximately 30% and due to urbanisation this percentage is increasing annually by 8% [1]. The significant energy demand results in higher contribution of greenhouse gas emissions. However, the energy saving potential of the building sector will result in impactful reduction of energy consumption. The incorporation of the passive techniques like cross ventilation, trombe wall, orientation, earth shelter, wind tower, shading etc. will curtail the energy demand. In view of this, the energy generation within the building by using photovoltaic (PV) modules is in the trend. But again, the creation of thermal energy during the conversion of low grade solar energy into electrical energy limits the efficiency of the PV systems [2]. Therefore, to make the thermal energy into usable form photovoltaic thermal (PVT) systems were developed, which increases the overall efficiency of PV systems [3]. At the same time, it also reduces the temperature of PV cells thereby increasing its conversion efficiency [4]. Many researchers have integrated PVT systems with building by using opaque PV modules to bring the generating unit near electrical and thermal load [5,6]. Further the researchers have found that for identical packing factor and dimension of semi-transparent PV (SPV) modules and opaque PV (OPV) modules, the former is more efficient. In addition to higher efficiency, SPV modules also provide daylighting. The integration of semi-transparent PV modules with buildings along with the provision to harvest the generated thermal energy is termed as building integrated photovoltaic thermal (BiSPVT) system. In consideration of energy savings, the responsible authority is watchful on reducing the transfer of heat by increasing the insulation levels [7]. However, in the region of temperate climate where summers are too hot, the use of BiSPVT system with high level of insulations reduces the occupant thermal comfort [8]. Yang and Tian [9] had found that solar shading

is a productive measure of increasing the comfort level since the glazed walls are usually the lowest performing part of building in controlling excess heat gain and energy loss. Many studies have suggested that by using optimal overhangs depth blocks solar beam irradiance of altitude sun trajectories in summer season and also allow the solar irradiance of low altitude sun trajectories in winter season. Thereby curtails the cooling load of summers and heating load demand of winters [10]. However, the solar diffuse irradiance are not blocked in summers due to which an occupant thermal comfort is compromised. On the other hand, movable insulation can be adjusted to block global solar irradiance in summer season and allow the global solar irradiance in winter season. Stazi et. al [11]found the potential of glazed walls in heating energy saving and thermal comfort in winter and intermediate seasons. Moreover, they suggested the use of double glazing to improve the performances. Further, the drawback of the glazing regarding the risk of overheating during summer season is also mentioned. Chen and Zheng [12] have analysed the feasibility of a microporous ceramic board based movable insulation in boilers to maintain a high constant temperature near the burner zone. Arinze et. al. [13] stated that in average climatic conditions, by using the movable thermal insulation between the double glazed greenhouses the heating requirement is reduced by as much as 60 to 80% in extremely cold regions. Yao [14] investigated the effect of movable insulation installed at south wall of a residential building on indoor thermal and visual comfort.

At present, there are only a few literatures on movable insulation installed in buildings which covers the vital thermal comfort. Furthermore, the performance of movable insulation is very much dependent on climatic condition. Hence the present work is done to bridge the gap between the use of MI in BiSPVT system and thermal comfort. A validated theoretical model has been developed for the BiSPVT system installed at Sodha BERS Complex (SBC), Varanasi, India.

**Table 1.** Nomenclature

| | | | |
|---|---|---|---|
| $U_{tca}$ | Overall heat transfer coefficient from top of SPV cell to ambient ($Wm^{-2}K^{-1}$) | $U_{sba}$ | Overall heat transfer coefficient from bricked side walls to ambient ($Wm^{-2}K^{-1}$) |
| $U_{bcr1}$ | Overall heat transfer coefficient from bottom of SPV cell to room ($Wm^{-2}K^{-1}$) | $U_{sga}$ | Overall heat transfer coefficient from glazed side walls to ambient ($Wm^{-2}K^{-1}$) |
| $h_{cfr1}$ | Convective heat transfer coefficient from floor to room ($Wm^{-2}K^{-1}$) | $U_{sga,MI}$ | Overall heat transfer coefficient from glazed side walls to ambient with MI ($Wm^{-2}K^{-1}$) |
| $U_{bcr2}$ | Overall heat transfer coefficient for floor to room 2 ($Wm^{-2}K^{-1}$) | C(ac) | Air conductance at various depth of cavity ($Wm^{-2}K^{-1}$) |
| α | Absorptivity | $V_1$ | Volume of room ($m^3$) |
| $\tau$ | Transmissivity | N | Number of air change of room |
| $\beta_m$ | Packing factor of SPV module | $\eta_m$ | Efficiency of SPV module |
| $\beta_k$ | Ratio of glass to total wall area | A | Area ($m^2$) |
| $M_{a1}$ | Mass of air in room (kg) | K | Thermal conductivity of materials ($Wm^{-1}K^{-1}$) |
| $C_{a1}$ | Specific heat of air in room ($Jkg^{-1}K^{-1}$) | L | Thickness of materials (m) |
| c | solar cell | gc | glass used in solar cell module |
| f | floor of room | gw | glass used in glazed side wall |
| g | Glass | bw | plastered brick used in wall |
| k | East, west , north, south | r | Roof formed by SPV modules |
| RCC | Reinforced cement concrete floor | 2 | Room-2 |
| cur | Curtain (Movable insulation) | 1 | Room |
| s | south | w | wall |

## 2. System description:

The schematic diagram of BiSPVT installed on the third floor (terrace) of Sodha BERS Complex (SBC), Varanasi, India is shown in Figure 1. The figure also outlines the dimensions, number of semi - transparent PV modules, glazing portion of side walls etc. In the present theoretical analysis, the temperature of room2 ($2^{nd}$ floor) underneath the room shown is taken constant because it is air conditioned. The reinforced cement concrete (RCC) beam structure is made to support the closed structure and withstand the heavy thrust of wind. The SPV modules are tightened with the RCC beams with the help of aluminium frame. The peak power rating of the system is 7.2 $kW_p$ ($75W_p \times 96$), which

has three power conditioning units (2 kVA, 48 V rating each), three set of batteries (48 V, 150 Ah rating each). The total area and ratio of glazed to bricked area of side walls facing east, west, north, south direction is given in Table 2. To remove hot air of the room, two exhaust fans (100 W, 220 V rating each) are installed.

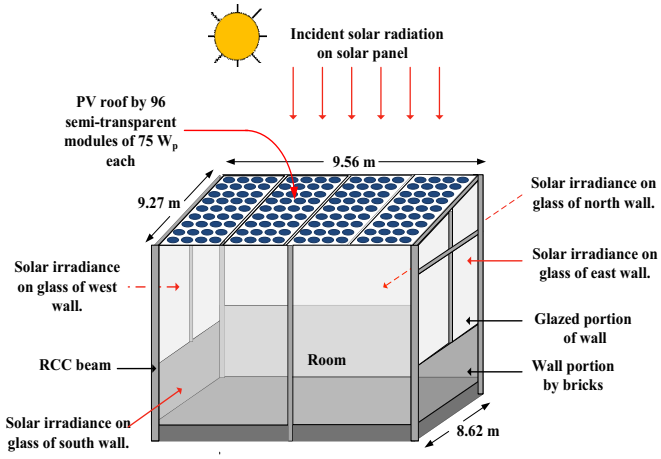


**Figure 1.** Schematic diagram of the BiSPVT system installed at Sodha BERS Complex, Varanasi.

**Table 2.** Design parameters and heat transfer coefficients

| Parameters | Values | Parameters | Values | Parameters | Values | Parameters | Values | Parameters | Values |
|---|---|---|---|---|---|---|---|---|---|
| $\beta_r$ | 0.05 | $L_{cur}$ | 0.003 | $K_{cur}$ | 0.06 | $A_r$ | 88.66 | $U_{sga,MI}$(0 ac) | 12.30 |
| $\beta_m$ | 0.85 | $L_{bw}$ | 0.1 | $\tau_g$ | 0.85 | $\alpha_c$ | 0.85 | $U_{sga,MI}$(1cm ac) | 4.03 |
| $\beta_e$ | 0.64 | $L_{gc}$ | 0.003 | $\eta_c$ | 0.09 | $\alpha_f$ | 0.6 | $U_{sga,MI}$(3cm ac) | 3.55 |
| $\beta_w$ | 0.44 | $L_{gw}$ | 0.004 | $A_f$ | 82.41 | $U_{tca}$ | 19.77 | C(1 cm ac) | 6 |
| $\beta_n$ | 0.12 | $K_{gc}$ | 1.1 | $A_e$ | 41.06 | $U_{bcr1}$ | 2.77 | C(3 cm ac) | 5 |
| $\beta_s$ | 1 | $K_{gw}$ | 1.1 | $A_w$ | 41.06 | $U_{sba}$ | 18.93 | | |
| $T_{r20}$ | 20 | $K_{bw}$ | 3.98 | $A_n$ | 64.13 | $U_{bcr2}$ | 4.7 | | |
| $L_{RCC}$ | 0.2 | $K_{RCC}$ | 1.28 | $A_s$ | 27.05 | $U_{sga}$ | 31.91 | | |

## 3. Thermal Modelling

The assumptions made for the development of theoretical thermal model are as follows:

- The heat is transfer from various nodes of the system namely SPV roof, side walls and floor is one dimensional and the system is in quasi-steady state.
- The thermal properties of the room air is constant with no stratification.
- The radiative heat transfer between walls and room is negligible due to small temperature difference.

The energy balance equations used in the formulation of theoretical model are as follows:

At cell of SPV module:

$$\alpha_c\tau_g\beta_m G_{inc} = U_{tca}(T_c - T_a) + U_{bcr1}(T_c - T_r) + \eta_m\,\tau_g\beta_m G_{inc} \quad (1)$$

At floor of the room:

$$\alpha_f\tau_g^2(1-\beta_m)(1-\beta_r)A_r G_{inc} + \alpha_f\tau_g\sum A_k\beta_k G_k = h_{cfr1}(T_f - T_r)A_f + U_{bcr2}A_f(T_f - T_{r20}) \quad (2)$$

At air of room:

$$h_{cfr1}(T_f - T_r)A_f + U_{bcr1}(T_c - T_r)\beta_m(1-\beta_r)A_r + (1-\alpha_f)\tau_g^2(1-\beta_m)(1-\beta_r)A_r\,G_{inc} + (1-\alpha_f)\tau_g\sum A_k\beta_k G_k = M_{a1}C_{a1}\frac{dT_r}{dt} + \sum A_k\beta_k U_k(T_r - T_a) + 0.33NV_1(T_r - T_a) \quad (3)$$

The Eq. (1)-(3) are solved to get the expression of $T_{r1}$ and $T_c$ as a function of input climatic parameters i.e solar irradiance and ambient air temperature. Hence,

$$\frac{dT_{r1}}{dt} + P_1 T_r = f(t) \quad (4)$$

$$\text{where, } f(t) = P_2 G_{inc} + X_3 \sum A_k \beta_k G_k + P_3 T_a + X_{40}$$

$$T_c = Z_1 T_a + Z_2 G_{inc} + Z_3 T_r \quad (5)$$

Eq. 4 is solved in MATLAB to get the expression of $T_r$. After getting the non-differential expression of $T_r$, the expression of SPV cell temperature ($T_c$) is evaluated with the help of Eq. 5. The details of expressions are defined in Appendix A and nomenclature.

**Table 3.** The obtained hourly experimental data for BiSPVT system on 19/Jan/2018.

| Time | 1 | 2 | 3 | 4 | 5 | 6 | 7 | 8 | 9 | 10 | 11 | 12 | 13 | 14 | 15 | 16 | 17 | 18 | 19 | 20 | 21 | 22 | 23 | 24 |
|---|---|---|---|---|---|---|---|---|---|---|---|---|---|---|---|---|---|---|---|---|---|---|---|---|
| $G_{inc}$ | 0 | 0 | 0 | 0 | 0 | 0 | 20 | 80 | 217.5 | 427.5 | 620 | 745 | 795 | 747.5 | 582.5 | 382.5 | 157.5 | 10 | 0 | 0 | 0 | 0 | 0 | 0 |
| $G_e$ | 0 | 0 | 0 | 0 | 0 | 0 | 110 | 320 | 517.5 | 622.5 | 562.5 | 367.5 | 200 | 150 | 125 | 95 | 55 | 15 | 0 | 0 | 0 | 0 | 0 | 0 |
| $G_w$ | 0 | 0 | 0 | 0 | 0 | 0 | 10 | 50 | 90 | 110 | 125 | 190 | 200 | 150 | 172.5 | 202.5 | 125 | 20 | 0 | 0 | 0 | 0 | 0 | 0 |
| $G_n$ | 0 | 0 | 0 | 0 | 0 | 0 | 5 | 15 | 32.5 | 37.5 | 42.5 | 47.5 | 50 | 50 | 47.5 | 42.5 | 27.5 | 7.5 | 0 | 0 | 0 | 0 | 0 | 0 |
| $G_s$ | 0 | 0 | 0 | 0 | 0 | 0 | 15 | 62.5 | 147.5 | 280 | 422.5 | 532.5 | 595 | 615 | 380 | 117.5 | 62.5 | 15 | 0 | 0 | 0 | 0 | 0 | 0 |
| $T_a$ | 16 | 15.6 | 15.1 | 14.5 | 13.5 | 12.5 | 12.3 | 13.7 | 15.8 | 18.3 | 21.3 | 23.8 | 25 | 25.5 | 25.9 | 25.6 | 24.1 | 22.5 | 21.5 | 20.3 | 19 | 18 | 17.24 | 16.5 |
| $T_{r,exp}$ | 17 | 16.5 | 16 | 15.5 | 15 | 14 | 14.2 | 17 | 19.3 | 22.1 | 24.9 | 26.5 | 27.9 | 28.9 | 28 | 27.2 | 23.2 | 22.8 | 22 | 21.4 | 20.4 | 19.8 | 18.8 | 17.8 |
| $T_{c,exp}$ | - | - | - | - | - | - | - | 17.2 | 25.2 | 35.3 | 41.1 | 42.9 | 45.4 | 43.8 | 37.2 | 32.4 | 23.9 | - | - | - | - | - | - | - |

## 4. Methodology:

(i) The hourly experimental data of solar irradiance (at inclined SPV roof, vertical side walls) and ambient air temperature were taken on Jan 19th 2018 by using solarimeter (Central electronic limited, India) and two laboratory thermometers (ZEAL, United Kingdom). The experiments were performed on Jan 19th 2018 at the site and the mentioned day was a clear day during the end of winter season in India. The experimental data is shown in Table 3.

(ii) To evaluate theoretical temperature of room ($T_r$) and SPV cell ($T_c$), computational codes were developed in the MATLAB 2015 software by using the thermal model described above.

(iii) The theoretical $T_r$ and $T_c$ were validated by the experimental data of the same which are also mentioned in Table 3. The hourly experimental data of $T_r$ and $T_c$ were taken by four laboratory thermometers (ZEAL, United Kingdom) and infrared thermometer (Fluke, U.S.A) respectively.

(iv) The good correlation between the experimental and theoretical temperatures validate the thermal model. Further, the effect of movable insulation on room and cell temperature were evaluated by using the thermal model.

(v) Moreover, to analyse the effect of MI in hot climatic condition of summer (Apr 03rd 2017, clear day) also, the computation has been done.

## 5. Result and discussion:

Figure 2 shows the hourly room air temperature on 19/Jan/2018 obtained through the theoretical model and experimental observations. The values of percentage root mean square deviation (e) and correlation coefficient (r) between the theoretical and experimental data are 6.43% and 0.99 respectively.

Figure 3 shows the hourly variation on 19/Jan/2018 of SPV cell temperature obtained theoretically

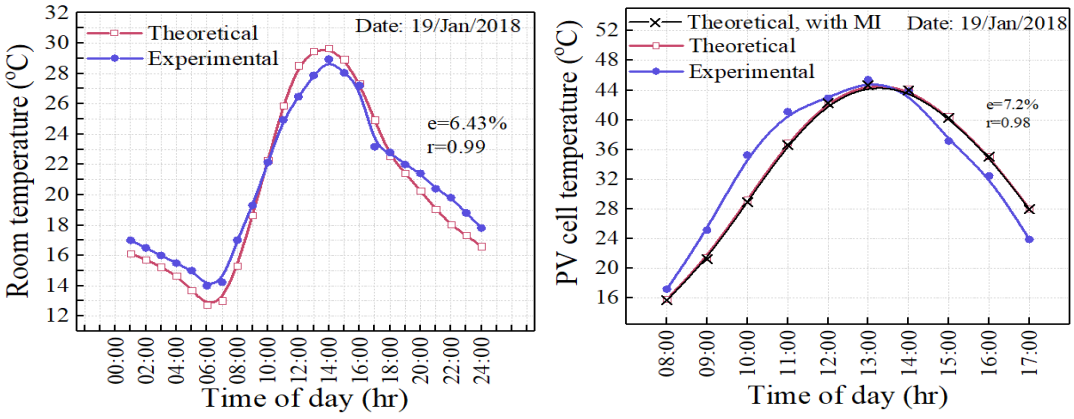

and experimentally. The variation of SPV cell temperature by applying movable insulation (MI) for intermittent duration i.e. 0700 to 1800 hour is also shown. By applying MI, the decrease in SPV cell temperature is negligible, thereby the increase in SPV electricity generation is marginal. The value of 'e' and 'r' are 7.2% and 0.98 respectively. The values of 'e' and 'r' shown in Figures 2 and 3 proofs the authenticity of the theoretical thermal model.

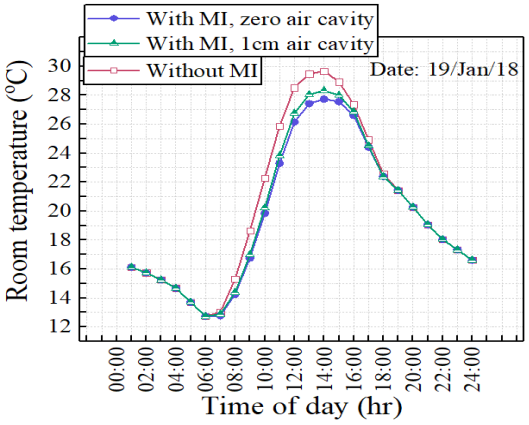


**Figure 4.** Effect of MI air cavity on the room temperature.

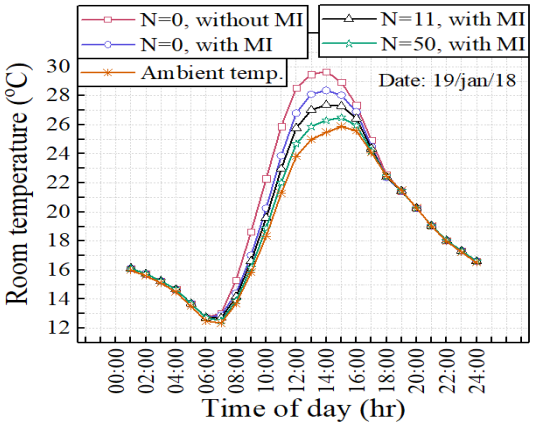


**Figure 5.** Effect of MI and number of air change on room temperature.

Through the validated thermal model, the effect of movable insulation on room temperature has been evaluated. The movable insulation (MI) is applied on glazed portion of side walls for intermittent duration (0700 to 1800 hours). Figure 4 depicts the plots of hourly room temperature of the BiSPVT system under various condition namely i) without MI, ii) with MI having zero air cavity and iii) with MI having 1 cm air cavity. The maximum temperature under the conditions are 29.66°C, 27.73°C and 28.32°C respectively. It has been found that MI with zero air cavity offers highest decrement in room temperature. This is because the glazed wall with zero air cavity has higher heat transfer coefficient ($U_{sga,MI}(0\ ac)$), hence the thermal conductance from room to ambient is higher in comparison to MI having 1cm ($U_{sga,MI}(1cm\ ac)$) air cavity.

Further, to decrease the room temperature the help of exhaust fan has been taken. Figure 5 shows the plots of hourly room temperature of the BiSPVT system under various condition namely i) number of air change (N)=0 and without MI, ii) N=0 and with MI, iii). N=11 and with MI and iv) N=50 and with MI. The MI used in this plots are with 3 cm air cavity ($U_{sga,MI}(3cm\ ac)$) and both N, MI are applied for intermittent duration as mentioned above. The maximum temperature under the conditions are 29.66°C, 28.37°C, 27.37°C and 26.30°C respectively. The decrement is observed with number of air change but it has also a limit that it cannot decrease the room temperature more than ambient temperature.

Further, the potential of MI combined with N to decrease the room temperature for a day in summer (03/Apr/2017) has been analysed as shown in Figure 6. The various conditions such as, MI material, depth of air cavity and applied duration of N/MI are the same as discussed in figure 5. The maximum temperature under the conditions are 43.68°C, 42.61°C, 41.32°C and 39.99°C respectively. By comparing the figures, it has been found that the decrement in room temperature by applying MI on 03/Apr/2017 is lesser in comparison to 19/Jan/2018 whereas the effect of number of air change is higher. Hence, the decrement offered by applying MI and N are very much dependent on climatic conditions.

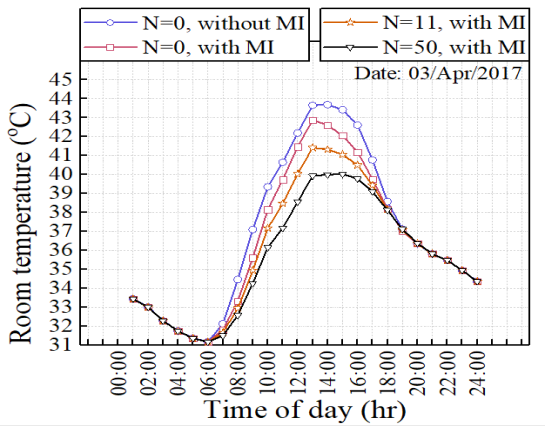

**Figure 6.** Effect of MI and number of air change on room temperature on 03/Apr/2017.

## 6. Appendix

$$S_2 = \sum_{k=e,w,n,s}\left[A_k U_{sga}\beta_k + A_k U_{sba}(1-\beta_k)\right] \quad A1$$

$$Q_2 = h_{cfr1}A_f + U_{bcr2}A_f \quad A2$$

$$Q_5 = h_{cfr1}A_f/Q_2 \quad A3$$

$$R_2 = 0.33NV_1 + S_2 \quad A4$$

$$A_c = A_r(1-\beta_r)\beta_m \quad A5$$

$$X_1 = R_2 - h_{cfr1}A_f Q_5 + h_{cfr1}A_f + U_{bcr1}A_c \quad A6$$

$$U_{tc} = U_{tca} + U_{br1} \quad A7$$

$$Z_3 = U_{bcr1}/U_{tc} \quad A8$$

$$X_5 = U_{bcr1}A_c/(M_{a1}C_{a1}) \quad A9$$

$$P_1 = X_1/(M_{a1}C_{a1}) - Z_3X_5 \quad A10$$

$$R_1 = (1-\alpha_f)\tau_g^2(1-\beta_m)(1-\beta_r)A_r \quad A11$$

$$Q_1 = \alpha_f\tau_g^2(1-\beta_m)(1-\beta_r)A_r \quad A12$$

$$Q_3 = Q_1/Q_2 \quad A13$$

$$X_2 = (h_{cfr1}A_f Q_3 + R_1)/(M_{a1}C_{a1}) \quad A14$$

$$Z_2 = \left(\alpha_c\tau_g\beta_m - \eta_c\tau_g\beta_m\right)/U_{tc} \quad A15$$

$$P_2 = X_2 + Z_2X_5 \text{ and } Z_1 = U_{tca}/U_{tc} \quad A16$$

$$X_6 = R_2/(M_{a1}C_{a1}) \text{ and } P_3 = Z_1X_5 + X_6 \quad A17$$

$$Q_4 = \alpha_f\tau_g/Q_2 \quad A18$$

$$X_3 = \left(h_{cfr1}A_f Q_4 + (1-\alpha_f)\tau_g\right)/(M_{a1}C_{a1}) \quad A19$$

$$Q_0 = U_{bcr2}A_f T_{r20} \quad A20$$

$$Q_{60} = Q_0/Q_2 \quad A21$$

$$X_{40} = (h_{cfr1}A_f Q_{60})/(M_{a1}C_{a1}) \quad A22$$

$$U_{tca} = \left[1/h_{0t} + L_{gc}/K_{gc}\right]^{-1} \quad A23$$

$$h_{0t} = 5.7 + 3.8\,v_{at},\ v_{at} = 4\ m/s \quad A24$$

$$U_{bcr1} = \left[1/h_{cfr1} + L_{gc}/K_{gc}\right]^{-1} \quad A25$$

$$h_{cfr1} = 2.8 + 3v_{r1},\ v_{r1} = 0\ m/s \quad A26$$

$$U_{bcr2} = \left[1/h_{cfr2} + L_{RCC}/K_{RCC}\right]^{-1} \quad A27$$

$$h_{cfr2} = 2.8 + 3v_{r2},\ v_{r2} = 5\ m/s \quad A28$$

$$U_{sga} = \left[1/h_{0s} + L_{gw}/K_{gw}\right]^{-1} \quad A29$$

$$U_{sba} = \left[1/h_{0s} + L_{bw}/K_{bw}\right]^{-1} \quad A30$$

$$U_{sga,MI} = \left[L_{cur}/K_{cur} + 1/C(dep) + 1/h_{0s} + L_{gw}/K_{gw}\right]^{-1} \quad A31$$

$$\text{where, } h_{0s} = 5.7 + 3.8\,v_{as},\ v_{as} = 8\ m/s \quad A32$$

## 7. References

[1] Babu K R and Vyjayanthi C 2017 Implementation of net zero energy building (NZEB) prototype with renewable energy integration *IEEE Region 10 Symposium (TENSYMP) 2017* pp. 1-5.
[2] Notton G, Cristofari C, Mattei M and Poggi P 2005 Modelling of a double-glass photovoltaic module using finite differences *Applied Thermal Engineering* Vol 25 pp. 2854 - 77.
[3] Kim J H and Kim J T 2012 A simulation study of air-type building-integrated photovoltaic-thermal system *Energy Procedia* Vol 30 pp. 1016 – 24.
[4] Chen F and Yin H 2016 Fabrication and laboratory-based performance testing of a building-integrated photovoltaic-thermal roofing panel *Applied Energy* Vol 177 pp. 271–84.
[5] Chow T T 2010 A review on photovoltaic/thermal hybrid solar technology *Appl. Energy* Vol 87 pp. 365–79.
[6] Agrawal B and Tiwari G N 2010 Optimizing the energy and exergy of building integrated photovoltaic thermal (BiPVT) systems under cold climatic conditions *Appl. Energy* 87 pp. 417–26.
[7] IEA. Technology roadmap - energy efficient building envelopes. International Energy Agency; 2013.
[8] Chvatal S K M and Corvacho H 2009 The impact of increasing the building envelope insulation upon the risk of overheating in summer and an increased energy consumption *Journal of Building Performance Simulation* Vol 2 pp. 267-82.
[9] Yu J, Yang C and Tian L 2008 Low-energy envelope design of residential building in hot summer and cold winter zone in China *Energy Buildings* Vol 40 pp. 1536-46.
[10] Feuermann D and Novoplansky 1998 A Reversible low solar heat gain windows for energy savings *Solar Energy* Vol 62 169-75.
[11] Stazi F, Mastrucci A and Perna C D 2012 The behaviour of solar walls in residential buildings with different insulation levels: An experimental and numerical study *Energy and Buildings* Vol 47 pp. 217–29.
[12] Chen D and Zheng C 2002 Experimental investigation on the feasibility of a movable heat-insulation device *Applied Thermal Engineering* Vol 22 pp. 1905–18.

[13] Arinze E A, Schoenau G J and Besant R W 1986 Experimental and computer performance evaluation of a movable thermal insulation for energy conservation in greenhouses, *Jour of agricultural Engineering* Vol 34 pp. 97-113.
[14] Yao J 2014 An investigation into the impact of movable solar shades on energy, indoor thermal and visual comfort improvements *Building and Environment* Vol 71 pp. 24-32.